



Substorm triggering by new plasma intrusion: Incoherent-scatter radar observations

L. R. Lyons,¹ Y. Nishimura,^{1,2} Y. Shi,¹ S. Zou,^{1,3} H.-J. Kim,¹ V. Angelopoulos,⁴ C. Heinselman,⁵ M. J. Nicolls,⁵ and K.-H. Fornacon⁶

Received 4 December 2009; revised 16 March 2010; accepted 30 March 2010; published 27 July 2010.

[1] In the companion paper, we identified a repeatable sequence of events leading to substorm onset in THEMIS all-sky imager observations: enhanced flows bring new plasma into the plasma sheet. The new plasma then moves earthward as a flow channel, bringing it to the near-Earth plasma sheet and where it produces onset instability. New plasma entering the dusk (dawn) convection cell drifts equatorward and eastward and then around the Harang reversal, leading to pre-midnight (near- and post-midnight) onset. Here we present evidence supporting this sequence using incoherent scatter radar (ISR) ionospheric observations. Using the Sondrestrom ISR, we find that enhanced flows of new plasma commonly enter the plasma sheet from the polar cap ~8 min prior to onset. These flows are related to poleward boundary intensification signatures, consistent with the inferences from the imagers. Using the Poker Flat ISR (PFISR), we find that shortly before onset, enhanced westward flows reach the subauroral polarization streams (SAPS) region equatorward of the Harang reversal (dusk-cell onsets) or enhanced eastward flows enter the onset region from the poleward direction (dawn-cell onset). PFISR proton precipitation signatures are consistent with the possibility that the enhanced flows consist of reduced-entropy plasma sheet plasma, and that onset occurs poleward of much of the enhanced SAPS flow (dusk-cell onsets) or equatorward of the enhanced eastward flows (dawn-cell onsets). Consistency with reduced entropy plasma is seen only within the enhanced flows, leading us to suggest that intrusion of low-entropy plasma may alter the radial gradient of entropy toward onset instability.

Citation: Lyons, L. R., Y. Nishimura, Y. Shi, S. Zou, H.-J. Kim, V. Angelopoulos, C. Heinselman, M. J. Nicolls, and K.-H. Fornacon (2010), Substorm triggering by new plasma intrusion: Incoherent-scatter radar observations, *J. Geophys. Res.*, *115*, A07223, doi:10.1029/2009JA015168.

1. Introduction

[2] Since the discovery of the substorm more than 40 years ago [Akasofu, 1964], determination of the sequence of events that leads to substorm onset has been a critical problem and the subject of much debate. A potential resolution to this long-term problem is given in the companion paper [Nishimura *et al.*, 2010], which reports a repeatable sequence of events

leading to substorm onset in observations from the THEMIS all-sky imager (ASI) array. Using the known relation between auroral enhancements and plasma sheet flows [e.g., *de la Beaujardière et al.*, 1994; Lyons *et al.*, 1999; Sergeev *et al.*, 1999, 2000; Nakamura *et al.*, 2001; Zesta *et al.*, 2002; Henderson *et al.*, 2002], the observed auroral sequence was used to suggest that new plasma crosses the polar cap boundary into the plasma sheet and then intrudes to the near-Earth region of the plasma sheet, leading to onset. It was also suggested that the intruding new plasma has lower flux tube entropy than the pre-existing plasma sheet plasma. (The flux tube entropy for an isotropic plasma is $\propto \log(PV^{5/3})$ [Wolf *et al.*, 2009], where P is pressure and V is flux tube volume.)

[3] As summarized by Nishimura *et al.* [2010, Figure 11], the pre-onset sequence starts with formation of a poleward boundary intensification (PBI) along the auroral poleward boundary, which lies nearly along the separatrix between open and closed magnetic field lines. An approximately north-south oriented (NS) auroral form then extends equatorward from the PBI toward the equatorward boundary of the aurora oval, which turns into enhanced auroral brightness that often drifts azimuthally (westward or eastward for

¹Department of Atmospheric and Oceanic Sciences, University of California, Los Angeles, California, USA.

²Solar-Terrestrial Environment Laboratory, Nagoya University, Nagoya, Japan.

³Department of Atmospheric, Oceanic and Space Sciences, University of Michigan, Ann Arbor, Michigan, USA.

⁴Department of Earth and Space Sciences, University of California, Los Angeles, California, USA.

⁵Center for Geospace Studies, SRI International, Menlo Park, California, USA.

⁶Institut für Geophysik und Extraterrestrische Physik, Technische Universität Braunschweig, Braunschweig, Germany.

auroral onsets in the dusk-cell or dawn-cell, respectively). Onset occurs when the enhanced auroral luminosity region reaches the onset location. Substorm onset can also be observed near the location where the NS auroral form first reaches a growth phase arc located near the equatorward boundary of the auroral oval.

[4] Auroral enhancements are expected to lie to the right of the direction of the associated enhanced flow channel, as illustrated in the ionosphere from *Nishimura et al.* [2010, Figure 11]. This is based on the enhanced upward field-aligned currents within the auroral enhancement being fed by enhanced ionospheric Pedersen currents within the flow channels. Onsets were observed to occur most commonly within the dusk convection cell. Such onsets are inferred to be associated with flows that start at the polar cap boundary, move toward the equatorward portion of the auroral oval, and then flow around the flow shear of the Harang reversal and enter the subauroral polarization streams (SAPS) region equatorward of that flow reversal. The auroral signatures of these onsets occur in the vicinity of the Harang reversal and near the poleward boundary of the SAPS (see *Bristow et al.* [2001, 2003], *Bristow and Jensen* [2007], *Bristow* [2009] and *Zou et al.* [2009a, 2009b] for discussions of these relationships).

[5] In this paper, we use ionospheric observations from two incoherent scatter radars (ISR) to obtain evidence for these inferred flows and consistency with the suggestion that the flowing magnetospheric plasma has lower $PV^{5/3}$ than the preexisting plasma. The Sondrestrom, Greenland ISR is used to look for evidence of pre-onset flows that cross the auroral poleward boundary prior to onset as well as for evidence of concurrent PBIs in the measured E region electron densities. The Alaskan ISR at Poker Flat (PFISR) is used to look for the azimuthal flows within the equatorward portion of the auroral oval shortly before onset. The PFISR observations of E region densities are also examined for evidence that the flowing plasma may have lower $PV^{5/3}$ than surrounding plasma.

2. Observational Approach

[6] Both radars were operated in modes selected to maximize latitudinal coverage and temporal resolution of flow measurements. Runs ~ 7 – 8 h in length were centered approximately at magnetic midnight. The mode selected for the nightside Sondrestrom ISR radar runs used by *Lyons et al.* [2009a] is identical to that for the dayside radar runs used by *Zou et al.* [2008] and *Kim et al.* [2009], except that the radar looked equatorward rather than poleward. This gives flow measurements versus invariant latitude Λ along the portion of the radar magnetic meridian equatorward of the radar location ($\Lambda = 74^\circ$, 24 MLT = 0225 UT), covering the most probable latitudes of the auroral poleward boundary found by *Nishimura et al.* [2010]. One complete radar cycle includes two scans, one looking east and one looking west, allowing line-of-sight (l-o-s) flow measurements to be obtained approximately along a magnetic meridian east of, and a magnetic meridian west of, the radar. Then the scan cycle is repeated. The F region velocities from each two nearest-in-time scans are combined to produce perpendicular velocity vectors. The velocity parallel to the magnetic field \mathbf{B} is assumed to be zero, and longitudinal homogeneity and temporal stability

between subsequent scans are assumed, as well. Finally, the resolved velocities are averaged in 0.25° latitude bins to reduce measurement error. This procedure gives flow vectors every ~ 2.5 min, although independent vector measurements are obtained every ~ 5 min, including the two 25 s transition intervals between the east and west scans. Observations from 64 nightside runs from December 2007 through March 2009 were available for this study.

[7] The operation mode for the nightside runs of PFISR used here is described by *Zou et al.* [2009b, 2009c] and *Lyons et al.* [2009b], and flow measurements along the radar magnetic meridian extend poleward from the radar location ($\Lambda = 65.4^\circ$, 24 MLT = 1115 UT). PFISR is a modern, phased array radar with the ability to steer on a pulse-to-pulse basis [*Heinselman and Nicolls*, 2008]. The radar operation mode selected for our studies of ionosphere-plasma sheet electrodynamic coupling consists of 13 beam directions, four each pointed toward westward azimuths, toward eastward azimuths, and at different poleward elevation angles along the magnetic meridian. One additional beam is directed along the local magnetic field. Some runs were done in a similar “world-day” mode, which is the same as the above mode except that the lowest-latitude eastward, westward, and poleward looking beams are absent. Vector velocities within the F region are calculated as a function of latitude along the radar magnetic meridian from the multiple l-o-s measurements within each latitude bin assuming that longitudinal variations within the radar field-of-view can be neglected [see *Heinselman and Nicolls*, 2008]. Observations from 88 nightside runs from March 2007 through May 2008 were available for this study.

3. Observation Examples

3.1. Sondrestrom Observations

[8] An example of the nightside Sondrestrom runs for a 3-h interval on 11 Feb 2009 is shown in Figure 1; the top four panels show the radar observations as a function of Λ and UT. The second, third, and fourth panels show the velocity direction, magnitude, and vector, respectively, within the F region, where collisions are sufficiently rare that the velocities are the electric field drift velocities. E region electron densities at 130 km altitude, which respond to auroral electron precipitation, are shown in the top panel. The low-density values and noisier data seen prior to ~ 02 UT are indicative of the low energy flux of precipitation expected along open polar-cap field lines. The high values seen from ~ 0207 – 0220 UT are the expected result of the high fluxes of electron precipitation corresponding to intense aurora, and the intermediate values seen after that time indicate less intense electron precipitation from the plasma sheet. We will use values below and above $\sim 3 \times 10^{10} \text{ m}^{-3}$ to indicate polar cap and plasma sheet, respectively, as was initially done with Sondrestrom radar observations by *de la Beaujardière et al.* [1991].

[9] Since our goal is to look for the pre-onset equatorward flow enhancements inferred by *Nishimura et al.* [2010], substorm onsets must be identified. Although auroral imaging is not available in the vicinity of Greenland for our events, our Sondrestrom runs were scheduled so that THEMIS spacecraft [*Angelopoulos*, 2008] were within the inner plasma sheet in roughly the same local time sector as the radar. To identify

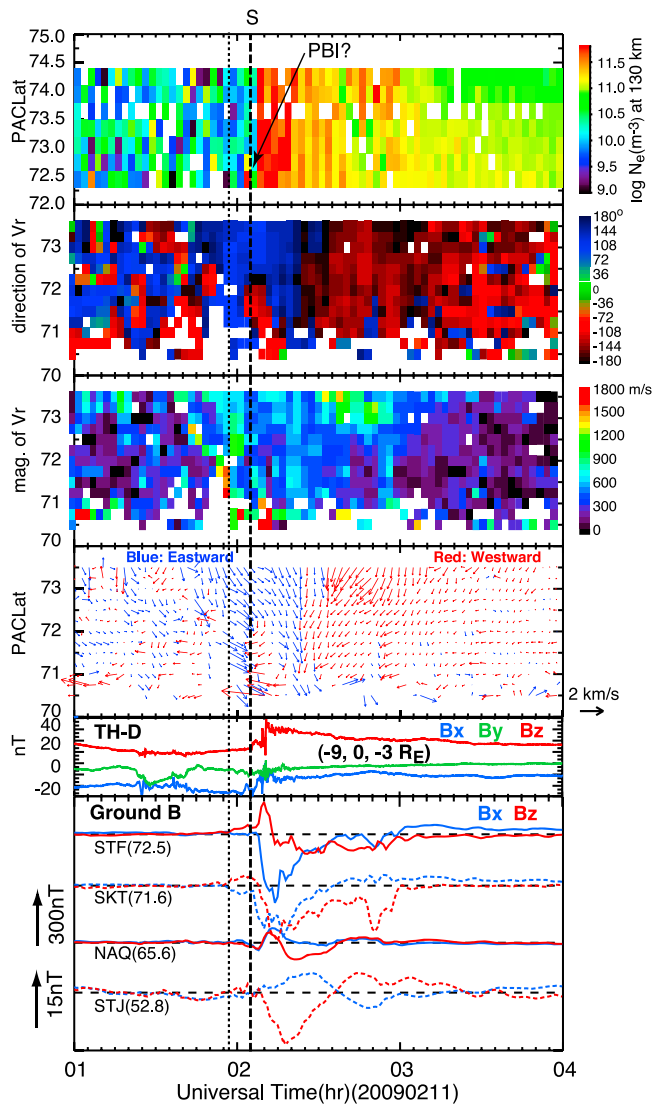


Figure 1. Observations from a 3-h interval during a Sondrestrom radar run on 11 February 2009. The second to fourth panels show, respectively, F region velocity direction, magnitude, and vector as a function of Λ and UT. E region densities at 130 km altitude as a function of Λ and UT are shown from each radar scan in the top panel. Values below and above $\sim 3 \times 10^{10} \text{ m}^{-3}$ indicate polar cap and plasma sheet, respectively. The three magnetic field components from the THEMIS D spacecraft and B_x and B_z from available Greenland magnetometers ground stations and Canadian midlatitude magnetometers nearest the Greenland meridian are shown in the bottom two panels to identify onsets of Figure 1. A vertical dashed line and “S” along the top of Figure 1 indicate the identified time of a substorm onset. The vertical dotted line identifies the initiation time of the observed pre-onset flow enhancement. A possible PBI signature is identified in E region density panel. The THEMIS spacecraft location at the center of the time interval in Figure 1 is given as (x,y,z) in GSM.

onsets, we therefore use magnetic dipolarization signatures observed with the THEMIS magnetometers [Auster *et al.*, 2008], as well as ground observations from all available Greenland magnetometers within the auroral zone and the Canadian midlatitude magnetometers STJ and OTT nearest the Greenland meridian. Midlatitude data from FRD and BOU were also examined though are not shown here. The three magnetic field components from the THEMIS D spacecraft and B_x and B_z from the ground stations are shown in the bottom two panels of Figure 1. The time of the earliest magnetic signature is identified as onset, which is accurate to ~ 1 – 2 min and is sufficient for our purposes.

[10] Figure 1 shows magnetic field dipolarization, as well as typical substorm ground magnetic signatures along the Greenland array and a midlatitude positive bay at STJ, all initiating at ~ 0205 UT. We thus choose ~ 0205 UT, indicated by a vertical dashed line and “S” along the top of Figure 1, as the time of a substorm onset. Before this time, the measured flows show a substantial enhancement directed toward the southeast. While some data are missing due to the low F region densities within the polar cap that occur during solar minimum conditions, at several latitudes the flow enhancement can be seen to initiate at 0157 UT, ~ 8 min prior to onset. This time, identified by a dotted line in Figure 1, is close to the average time before onset that Nishimura *et al.* [2010] reported the intensification of a PBI (~ 5.5 min).

[11] As seen in Figure 1, the entire E region field-of-view (fov) of the radar ($\Lambda \sim 72.3^\circ$ to 74.3°) was within the polar cap when the flow enhancement was first observed, and enhanced flows were observed up to the poleward edge of the radar F region fov ($\Lambda \sim 73.5^\circ$). Thus, the flow enhancement gave enhanced plasma transport across polar cap field lines toward the plasma sheet, as previously observed by de la Beaujardière *et al.* [1994] for flows associated with PBIs. Consistent with association of the enhanced flows in Figure 1 with a PBI, a brief enhancement of E region densities was seen near $\Lambda \sim 72.5^\circ$ just before the identified substorm onset time. (The enhanced E region densities seen ~ 2 min after onset likely correspond to poleward expansion of the substorm auroral bulge.) It should be noted that the time when a flow enhancement crosses the polar cap boundary is the most appropriate for comparison with the inferences of Nishimura *et al.* [2010]. There was a southeastward-directed flow enhancement at the highest latitude measured (72.3°) near 0147 UT, but the flow enhancement at this time did not extend toward the polar cap boundary. On the other hand, the flow enhancement at 0157 UT extended to the equatorward boundary of the radar F region fov, and thus likely crossed the polar cap boundary at about that time.

[12] While the transition to plasma sheet E region densities was equatorward of the radar E region fov at this time, the F region flow enhancement is seen to extend $\sim 2^\circ$ equatorward of the E region fov, so the enhanced flows likely crossed the open-close field line boundary as observed by de la Beaujardière *et al.* [1994]. These flows likely enhanced transport of plasma lying along polar cap field lines into the plasma sheet, providing new plasma to the plasma sheet. In particular, mantle plasma carried across the polar cap by the electric drift and to the distant plasma sheet is believed to be an important source for the plasma sheet [Pilipp and Morfill, 1978; Maezawa and Hori, 1998]. Enhancement of the electric drift would increase such entry of mantle plasma. The

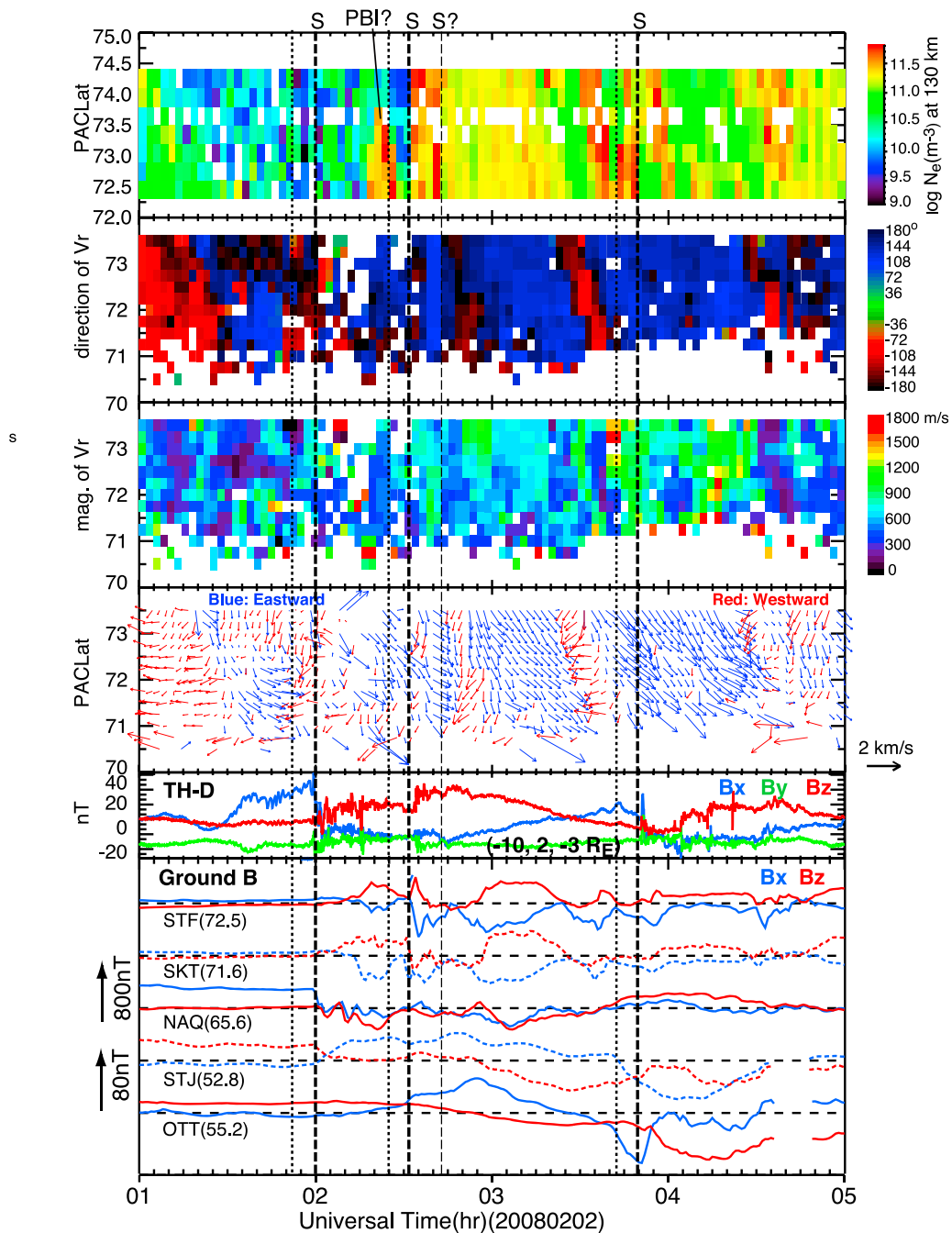


Figure 2. Observations from a 4 h interval during a Sondrestrom radar run on 2 February 2008 in the same format as Figure 1.

enhanced flow across the polar-cap boundary also corresponds to an increase in the local reconnection rate [de la Beaujardière *et al.*, 1991; Blanchard *et al.*, 1996]. It is interesting that the flow enhancement produces an ionospheric current enhancement sufficiently large to cause observable magnetic perturbations at the two highest-latitude Greenland stations shown in Figure 1, STF and SKT.

[13] Figure 2 shows observations from a 4 h interval on 2 February 2008. During this period the THEMIS D spacecraft observed three clear dipolarizations marked by thick dashed lines in Figure 2, and possibly another dipolarization at 0243 UT identified by a lighter dashed line. The first

two dipolarizations have concurrent magnetic signatures in Greenland stations and positive bays at STJ, the nearest to the Greenland meridian of the two midlatitude stations shown, and at OTT for the second event. Positive bays are also seen for the 0243 UT possible dipolarization and at the further to the west station OTT for the 0350 UT onset that occurred post midnight in Greenland. Flow enhancements preceded all four events by several minutes. The first was mostly southward, with some deflection toward the west; the others were southeastward as was the enhancement on 11 Feb 2009. The first flow enhancement was seen within the polar cap, and the *E* region densities show evidence for a

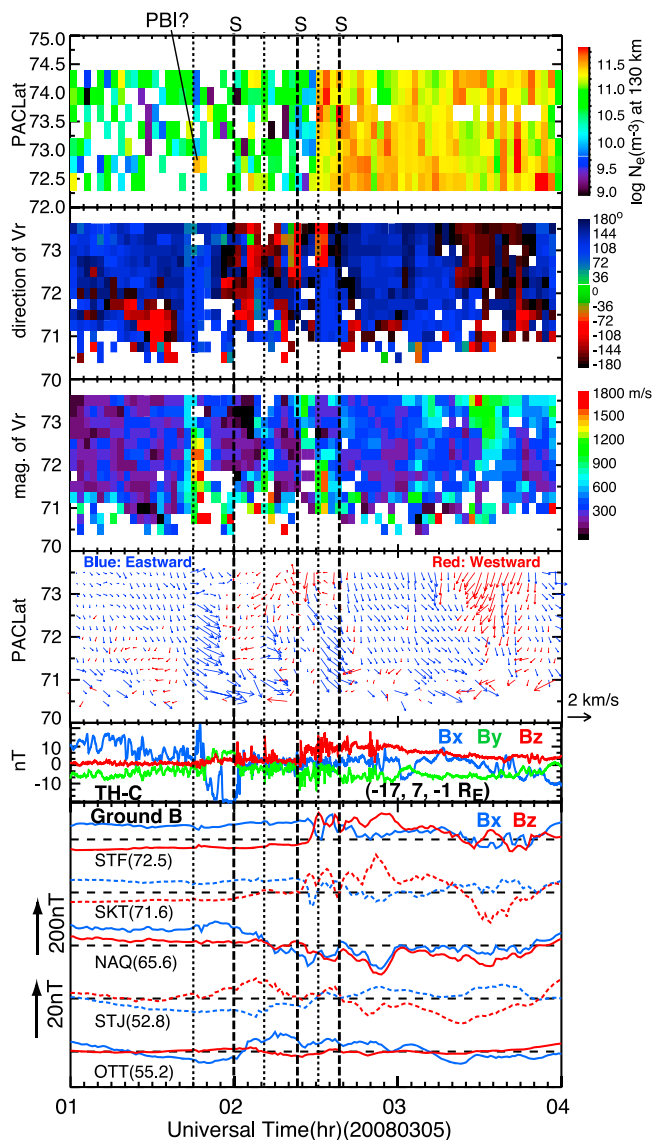


Figure 3. Observations from a 3 h interval during a Sondrestrom radar run on 5 March 2008 in the same format as Figure 1.

PBI associated with the flow enhancement preceding the second onset. Also, there are other flow enhancements that we have not associated with the identified onsets, such as those starting at ~ 0140 and ~ 0330 UT which end before the identified onsets. Such flow enhancements are expected, since there are many PBIs that are not associated with substorm onsets.

[14] Three particularly clear southeastward-directed flow enhancements preceding three onsets on 5 March 2008 are shown in Figure 3, the first being associated with a possible PBI signature. Note that the polar cap boundary can be located out of the radar E region fov, and PBIs are expected to lie near the western edge of flow enhancements, and not within their centers. Thus, we do not expect to see evidence of a PBI for all flow enhancements seen in observations such as these that are made along one magnetic meridian.

[15] We identified a total of 36 substorm onsets during the examined runs of the Sondrestrom radar, and we identified a

flow enhancement as in the above example within 15 min of onset for 19 events. In three events flow enhancement was observed a few minutes earlier than 15 min before onset, perhaps too early to be associated with a PBI and an NS aurora that led to an onset. We saw flows without enhancement for only 6 onsets, with 1 additional case being ambiguous. For the remaining 7 events, low electron densities prior to onset prevented reliable flow measurements. More than one flow burst can cross the near midnight polar cap boundary prior to an onset, however, and many flow bursts are not associated with onsets. Without an ASI array such as used by *Nishimura et al.* [2010], we cannot tell whether any individual flow enhancement we observed with the Sondrestrom radar led to the ensuing onset. Nevertheless, we can conclude that flow enhancements are commonly seen within the same range of times ΔT before onset, as inferred by *Nishimura et al.* [2010]. Also, the median ΔT (8 min) for the events seen within 15 min of onset is approximately the same as seen by *Nishimura et al.* [2010] (~ 5.5 min). These observations are thus consistent with *Nishimura et al.*'s [2010] inference that flow enhancements bringing new plasma across the outer plasma sheet boundary to the plasma sheet lead to onset.

3.2. PFISR Observations

[16] The PFISR fov covers the latitudes of some substorm auroral onsets. During the runs, we identified 4 events in which substorm onset occurred very close to or within this fov. Figure 4 shows a sequence of high-resolution auroral images from the THEMIS ASIs [*Mende et al.*, 2008] at Ft. Yukon (located near the center of the PFISR fov) and INUV, the next station to the east. Thin solid lines are shown at $\Lambda = 60^\circ$ and 70° , and thin dashed lines at $\Lambda = 65^\circ$ and 75° . Thin solid lines are also drawn every 15° in longitude, and a blue line is drawn at magnetic midnight in each image. The images show auroral evolution associated with a substorm on 12 December 2007. Prior to onset, there was a growth-phase arc at $\Lambda \sim 67^\circ$ (the bright region in the INUV imager fov is light contamination). A PBI brightening was first discernible at 10:21:24 UT near the western edge of the Ft. Yukon imager fov. The PBI can be seen to have connected to the equatorward growth phase aurora by an NS auroral structure by 10:22:12 UT, and the NS structure moved eastward after that to near the central meridian of the Ft. Yukon fov and the PFISR longitude. In the 10:27:36 UT image, onset can be seen, followed by poleward expansion, which can also be seen in the INUV images despite the light contamination.

[17] PFISR observations from 0950 to 1050 UT on 12 December 2007 are shown in Figure 5. The top three panels show the F region velocity direction, magnitude, and vector, respectively. Electron densities along one of the beams directed poleward along the magnetic meridian and the beam looking up along the local magnetic field direction are shown in the fourth and fifth panels, respectively. Altitude is shown along the left axis and Λ along the right axis. Ground magnetic observations are shown for three stations approximately along the radar meridian from Poker Flat (POKR) to Ft. Yukon (FYKN); Pi2 observations from POKR can be seen in the bottom panel. The time of the substorm onset identified in the imager observations of Figure 4 is indicated by a solid vertical line, and the latitude of initial substorm brightening is indicated by a star in the flow vector panel. The magnetic Z -component at FYKN and BETT shows negative pertur-

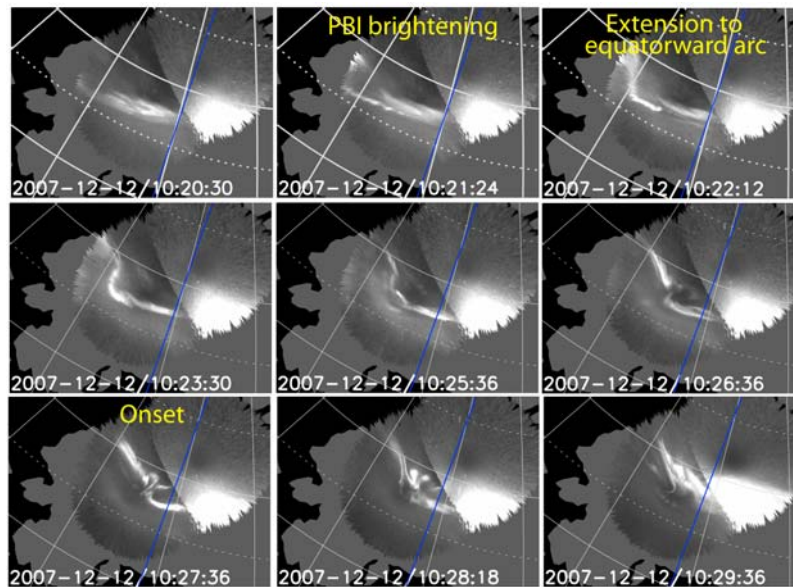


Figure 4. A sequence of high-resolution auroral images from the THEMIS ASI at FYKN (west) and INUV (east) associated with a substorm on 12 December 2007. Thin solid lines are shown at $\Lambda = 60^\circ$ and 70° and thin dashed lines at $\Lambda = 65^\circ$ and 75° . Thin solid lines are also drawn every 15° in longitude, a blue line being drawn at magnetic midnight in each image.

bations initiating at the onset time. This indicates that the westward electrojet formed with a center poleward of those stations, which is consistent with the westward electrojet being poleward of the onset latitude as seen by *Zou et al.* [2009b]. A positive H bay initiated at the lowest two latitude stations (BETT and POKR) at the same time; such bays have been attributed to an enhanced eastward current developing equatorward of the onset latitude [*Ritter and Lühr, 2008; Zou et al., 2009b*].

[18] Generally, electrons pitch angle scattered from the plasma sheet are the major source of nightside *E* region ionization. By using the Chatanika ISR and polar-orbiting satellite measurements, however, *Robinson and Vondrak* [1985] found that at times such ionization can be primarily due to precipitating protons. They showed that electron precipitation leads to ionization that falls off slowly from the peak density in the *E* region up to 200 km, a result further confirmed by quantitative calculations based on a physical model by *Smirnova et al.* [2004]. *Robinson and Vondrak* [1985] found that proton precipitation gives a far sharper ionization peak in the *E* region, as is seen at ~ 125 km by the beam directed up the magnetic field (beam 11) throughout the period shown in Figure 5 (except perhaps for the measurement point at 1000 UT). This sharp peak, consistent with proton precipitation, is also seen during most of the period shown for the poleward looking beam 10, effects of electrons likely being seen at ~ 1000 – 1005 , ~ 1020 , and ~ 1035 UT. That such a sharp ionization peak results from proton precipitation was further confirmed by *Zou et al.* [2009b] by using precipitating particle observations from a pass of the NOAA-17 spacecraft near the PFISR meridian.

[19] Due to the westward magnetic drift of protons and the eastward drift of electrons, proton precipitation often occurs equatorward of the inner edge of electron precipitation at pre-midnight MLTs. This is the region of strong westward

flows, referred to as SAPS [*Anderson et al., 1993, 2001, Foster and Burke, 2002*]. SAPS, which are commonly seen equatorward of the inner edge of plasma sheet electrons during the growth phase of substorms [*Lyons et al., 2009a; Zou et al., 2009a, 2009b*], have been found to respond substantially to substorm expansion phase onset [*Zou et al., 2009a, 2009b; Nishimura et al., 2008*]. In this particular case, although SAPS were not observed well before onset within the PFISR *F* region fov, they can be seen as enhanced westward flows initiating a few minutes before onset in the poleward portion of the fov.

[20] To look more carefully at these westward flows, Figure 6a shows *F* region l-o-s flow speeds versus UT. Using observations from all 4 of the westward-looking beam directions, flows are plotted at 8 different latitudes extending over the entire radar *F* region fov. Positive values indicate flows away from the radar. Dotted lines give 0 flow speed for each latitude. Showing l-o-s speeds avoids any ambiguities in the derived flow vectors that might arise from lack of longitudinal homogeneity and allows for accurate timing of flow enhancements. While the l-o-s directions are oriented somewhat to the north of pure west, the flow vectors in Figure 5 indicate that the flow enhancements are close to being purely westward.

[21] The flows in Figure 6a turn toward positive values beginning at ~ 1024 UT, a few minutes prior to onset, and they become substantially positive before onset. Such flows are expected from plasma intruding to the inner plasma sheet from the polar cap boundary, flowing around the Harang reversal and turning westward. The westward flow enhancement before onset is seen at all latitudes above 66.4° but not at lower latitudes (below 66.2°). A further enhancement is seen after onset, including at lower latitudes, consistent with the SAPS flow response to onset identified by *Zou et al.* [2009a, 2009b].

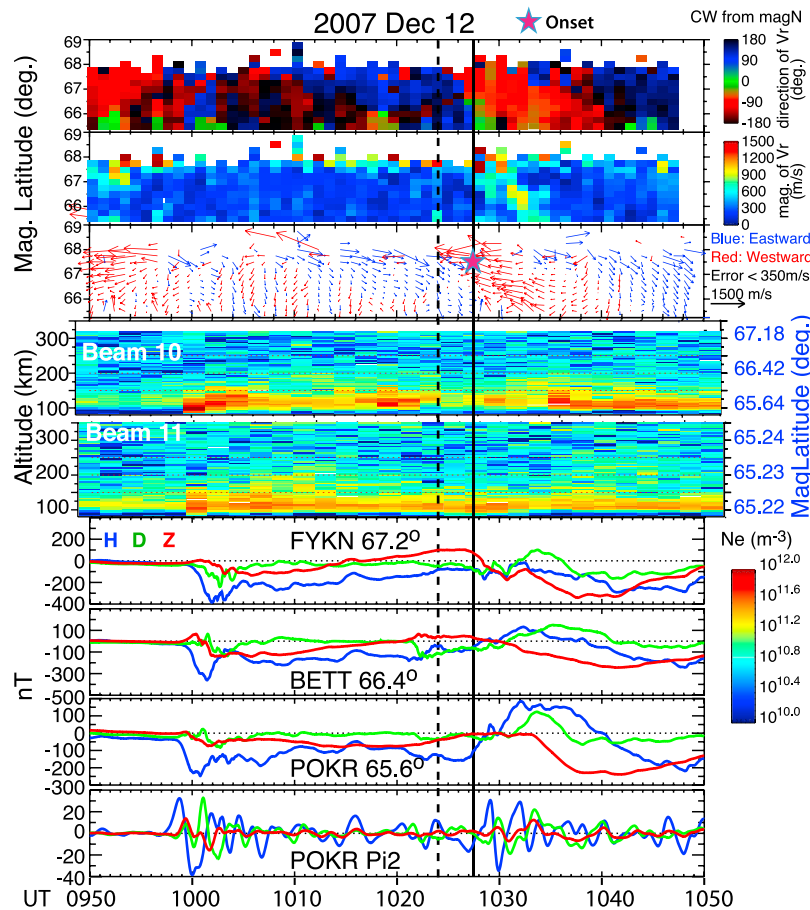


Figure 5. PFISR observations from 0950 to 1050 UT on 12 December 2007. The top three panels show F region velocity direction, magnitude, and vector, respectively. Electron densities along one of the beams directed poleward along the magnetic meridian and the beam looking up along the local magnetic field direction are shown in the fourth and fifth panels, respectively, altitude being shown along the left axis and Λ along the right axis. Ground magnetic observations are shown from POKR, BETT, and FYKN approximately along the PFISR meridian. Pi2 pulsations from POKR are shown in the bottom panel. The time of the identified substorm onset is indicated by a solid vertical line; the latitude of initial substorm brightening is identified by a star in the flow vector panel. The vertical dashed line represents the initiation time of the observed pre-onset flow enhancement.

[22] Figure 6b shows the E region densities for 8 different latitudes over the entire extent of the radar E region fov, the individual line colors matched to the color of the closest latitude of the F region speeds in Figure 6a. A clear density decrease can be seen to have initiated near the same time as the pre-onset positive turning of the l-o-s velocities in Figure 6a, and only at the same latitudes ($>66.2^\circ$) where the positive turning was observed. This density decrease is not seen at the lower latitudes where the flow speed enhancement was not observed until after onset, but instead increased resulting in an equatorward directed density gradient. Since the E region densities at these latitudes, below the region of electron precipitation, are likely the result of proton precipitation, they indicate that plasma brought to the radar fov by the enhanced westward flow led to a reduced energy flux of precipitating protons.

[23] Based on their observed pitch angle distributions [Stiles *et al.*, 1978; Nakamura *et al.*, 1991], the thermal population of plasma sheet protons is typically assumed to undergo

strong pitch angle scattering due to non-adiabatic motion within the tail current sheet. If we make this assumption, then the substantial reduction in the energy flux of precipitating protons would indicate a substantial reduction in the energy density of the plasma sheet proton population along the field lines of the E region density reduction. If we make the further assumption that the flux tube volume does not abruptly increase substantially at the same time (which we believe is reasonable, since the magnetic field within flow channels has been reported to be more dipolar than within surrounding regions [Angelopoulos *et al.*, 1992]), we find that the E region density decrease is consistent with the suggestion of Nishimura *et al.* [2010] that the new plasma entering the plasma sheet and reaching the near-earth region has lower $PV^{5/3}$ than the surrounding plasma.

[24] Note also that the flow enhancement and E region density decrease in Figure 6 is seen at latitudes extending from the poleward edge of the radar fov to $\sim 66.3^\circ$. These latitudes extend well equatorward of the auroral onset. Thus,

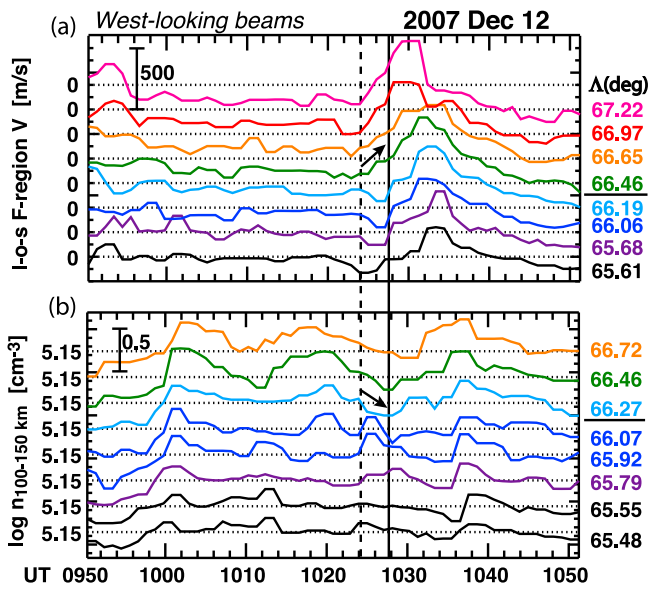


Figure 6. (a) *F* region I-o-s flow speeds versus UT obtained from westward-looking beams from 0950 to 1050 UT on 12 December 2007. Flows are shown at 8 different latitudes, identified along the right axis, covering the extent of the radar *F* region fov. Positive values indicate flows away from the radar. Dotted lines, which give 0 flow speeds for each latitude, are displaced upward by 200 m/s for each of the subsequently higher latitudes shown. (b) *E* region densities obtained from westward looking beams for 8 different latitudes extending over the extent of the radar *E* region fov, the individual line colors matched to the color of the closest latitude of the *F* region speeds in Figure 6a. The curve for each latitude is displaced upward by 0.3 in log n.

the auroral brightening at onset, which occurred at $\sim 67.5^\circ$, was poleward of at least some of the new plasma brought in by the enhanced flow. The observations suggest the possibility that the upward field-aligned currents of the auroral onset form near the poleward edge of the flows, as sketched by *Nishimura et al.* [2010, Figure 11] for onsets within the evening-side convection cell. This would be expected if the upward current is fed at least partially by poleward Pedersen currents associated with the enhanced flows in the SAPS region equatorward of the onset latitude.

[25] Figure 7 shows a sequence of high-resolution auroral images from the Ft. Yukon ASI on 13 March 2008. Despite light contamination from the Moon and another source to the east, as well as somewhat hazy viewing conditions, a growth-phase arc can be identified prior to onset at $\Lambda \sim 68^\circ$. A PBI, first discernible in the 10:00:00 UT image just west of the center of the imager fov might have initiated earlier but not been visible due to the viewing conditions. The PBI can then be seen to extend equatorward toward the growth phase arc leading to onset, which is first seen as gradual brightening of the onset arc in the 10:02:00 UT image.

[26] An overview of the PFISR observations from 0910 to 1010 UT on 13 March 2008 is shown in Figure 8 in the same format as Figure 5, an onset being marked with a star at $\Lambda \sim 68.5^\circ$. Only weak ground magnetic field responses are seen for this event, there being small negative H and positive Z perturbations at the most poleward station shown (KAKT, $\Lambda \sim 71.1^\circ$) and a Pi2 pulsation enhancement. As do the electron densities in Figure 5, the electron densities for the two poleward looking beams shown in Figure 8 (beams 10 and 13 at a lower and a higher elevation angle, respectively) also show the characteristics of pure proton precipitation as expected in the region equatorward of the onset. Westward SAPS flows can be seen prior to onset in this case starting within the highest latitude portion of the *F* region fov at ~ 0948 UT.

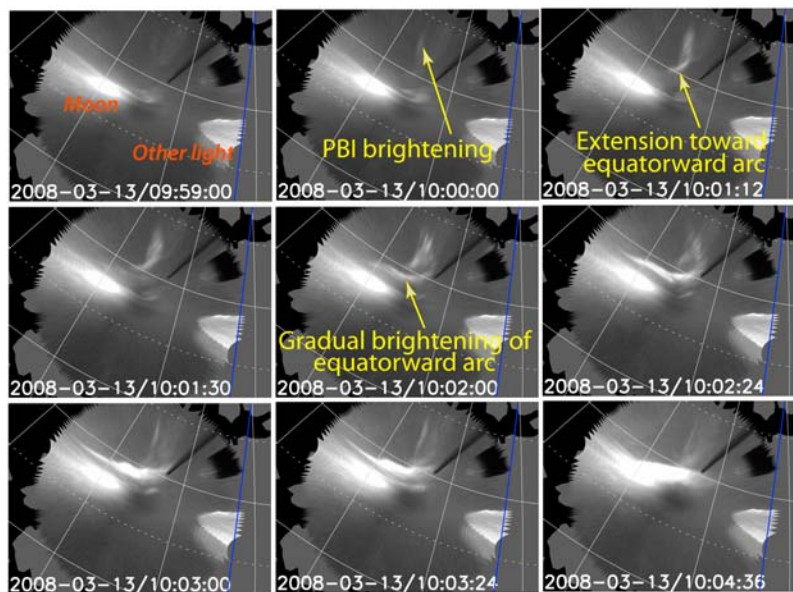


Figure 7. A sequence of high-resolution auroral images from the THEMIS ASI at FYKN associated with a substorm on 13 March 2008 in the same format as Figure 4.

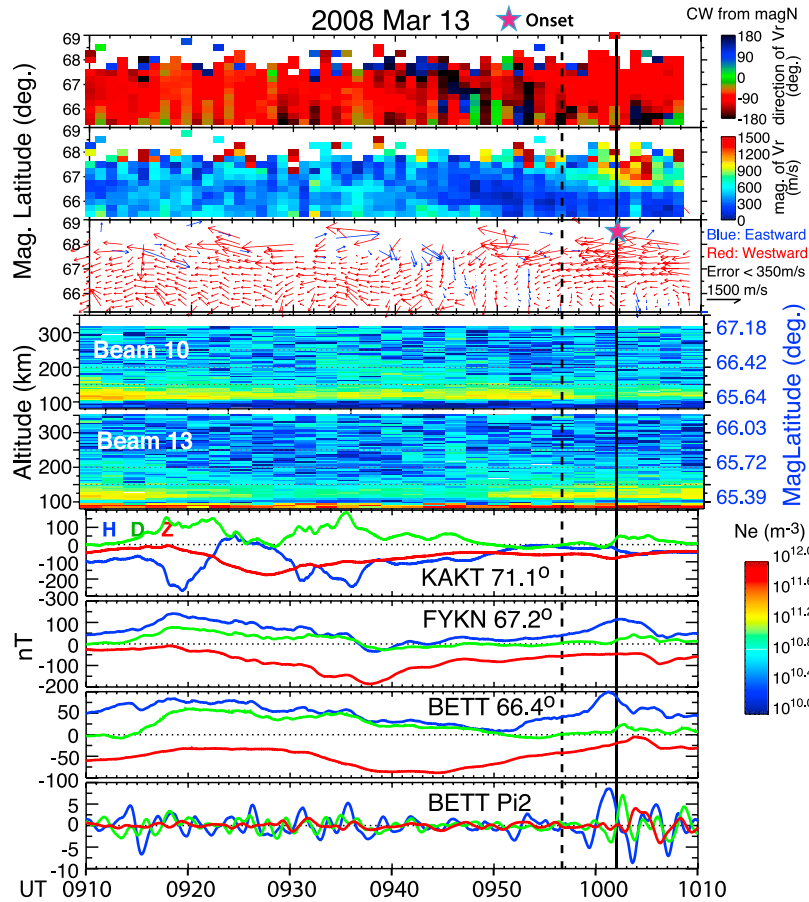


Figure 8. PFISR observations and ground magnetic observations from 0910 to 1010 UT on 13 March 2008 in the same format as Figure 5, except that electron densities along two of the beams directed poleward along the magnetic meridian are shown.

[27] Figure 9a shows *F* region l-o-s flow speeds versus UT for the same 8 latitudes shown in Figure 6a. As in Figure 6a, a turn toward positive values began prior to onset, at ~0956 UT. This westward flow enhancement before onset is seen at all latitudes above 66.4° but not at lower latitudes (below 66.2°), and some further enhancement is seen after onset. Figure 9b shows the *E* region densities for the same 8 latitudes as in Figure 6b. As for the example in Figure 6, a clear decrease in density began at nearly the same time as the positive turning of the l-o-s velocities and only at the same latitudes (>66.2°) at which the positive turning was observed. As in the previous example, the density decrease led to an equatorward-directed density gradient. This density decrease is again consistent with the suggestion that the plasma brought to this region by enhanced flows has lower $PV^{5/3}$ than the previous particle population. Also, as for the previous example, the auroral brightening at onset, which occurred poleward of at least some of the new plasma brought in by the enhanced flow, is consistent with the possibility that upward field-aligned currents formed at onset near the poleward edge of the flows.

[28] The final example of PFISR observations (onset at 0725 UT on 4 September 2008) is shown in Figure 10. Although good imaging was not available for this event, the time and latitude of the onset (shown in Figure 10) were

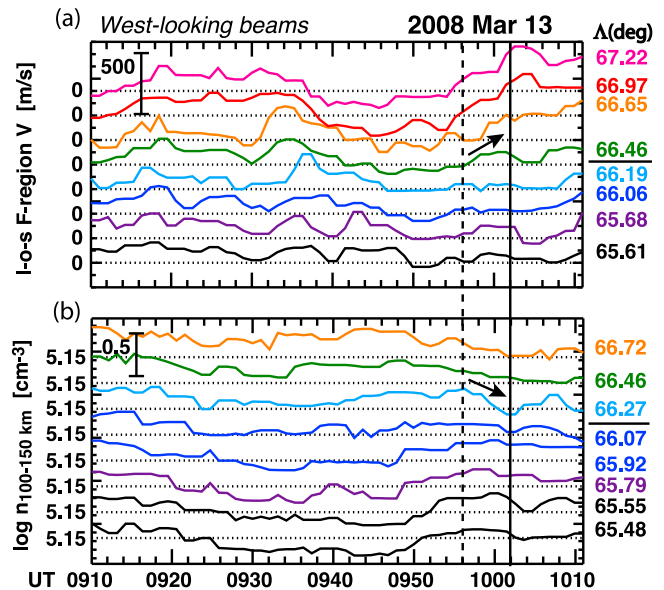


Figure 9. (a) *F* region l-o-s flow speeds and (b) *E* region densities versus UT obtained from westward looking beams from 0910 to 1010 UT on 13 March 2008 in the same format as Figure 6.

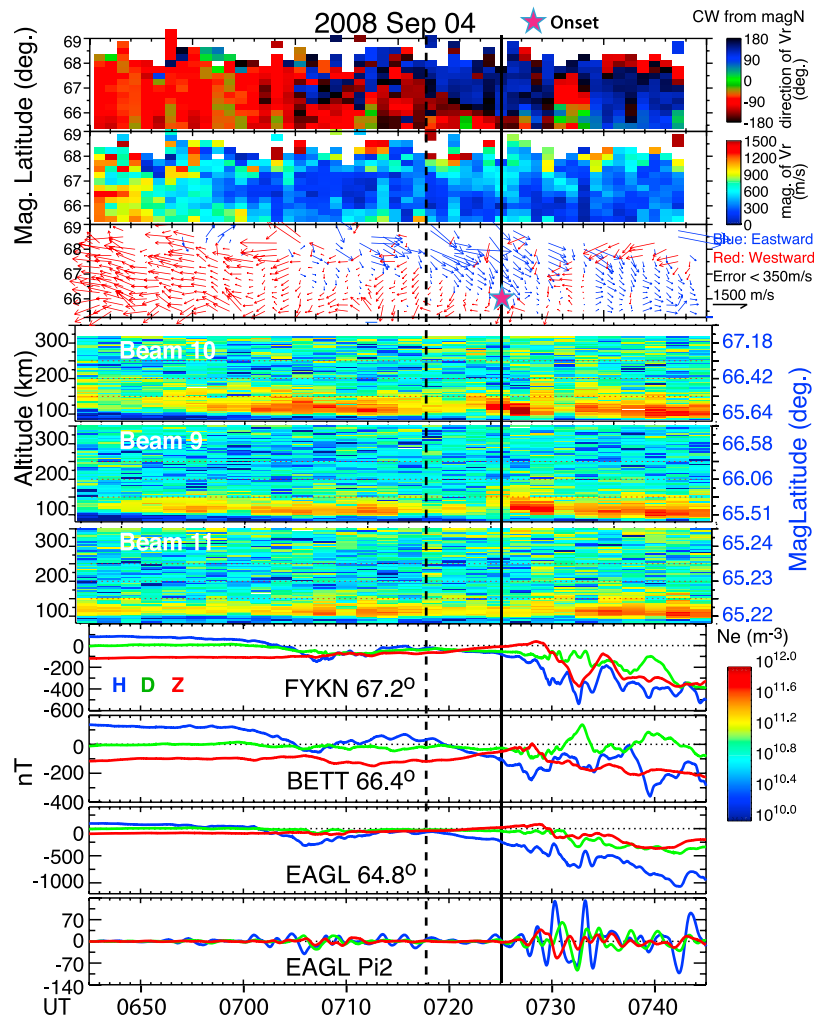


Figure 10. PFISR observations and ground magnetic observations from 0910 to 1010 UT on 13 March 2008 in the same format as Figure 5, except that electron densities along two of the beams directed poleward along the magnetic meridian and the beam looking up along the local magnetic field direction are shown.

determined by *Zou et al.* [2009b]. The onset was at $\Lambda \sim 66^\circ$. The densities prior to the onset in Figure 10 give evidence of pure proton precipitation at latitudes $\sim 0.5^\circ$ to $\sim 0.8^\circ$ equatorward of the onset.

[29] The flows in this case are different from those in the previous two cases. The previous cases are the most common type reported by *Nishimura et al.* [2010] (an auroral enhancement moves westward equatorward of the center of the Harang flow shear to an onset location within the evening side convection cell). However, in this case, starting at ~ 0710 UT, eastward flows can be seen in the poleward portion of the radar fov and westward flows at lower latitudes, indicating the Harang reversal. Then, starting at ~ 0718 UT, a southeastward-directed flow enhancement moves equatorward and reaches the onset latitude at approximately the onset time. This corresponds to the cases of *Nishimura et al.* [2010] in which onset occurs just when the equatorward-moving, NS-oriented auroral structure contacts the growth phase proton aurora. Onset occurs at the equatorward edge of the incoming southeastward-directed flow for this case.

As for the above cases, the flow direction is consistent with enhanced Pedersen currents driven by flows feeding at least a portion of the upward currents of the auroral onset, as sketched by *Nishimura et al.* [2010, Figure 11] for onsets within the dawn-side convection cell.

[30] In Figure 11, F region l-o-s flow speeds and E region densities from the westward-looking beams are shown for this event at the same 8 latitudes as shown in Figures 6 and 9. Since the flow increase is in the southeastward direction, the enhancement is seen as increasingly negative speeds. This increase can be seen at all latitudes above 66.1° , which is down to approximately the onset latitude. A perturbation in the negative direction is also seen at lower latitudes where the flows were initially westward. The E region densities decrease at all but the highest latitude; the decrease initiates at approximately the same time as the negative flow change. Except for the highest latitude, this is what would be expected if the plasma brought to this region by the enhanced flows had lower $PV^{5/3}$ than the previous plasma population. Note that the E region densities are seen to decrease prior to onset

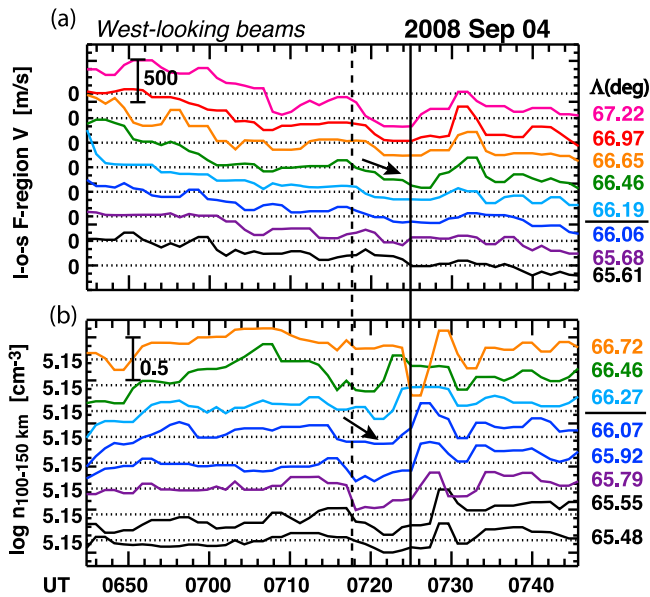


Figure 11. (a) F region l-o-s flow speeds and (b) E region densities versus UT obtained from westward looking beams from 0910 to 1010 UT on 4 September 2008 in the same format as Figure 6.

equatorward of the onset latitude, which indicates the possibility that lower $PV^{5/3}$ plasma was brought to this region as was seen for the two examples discussed above.

[31] In this case, however, the densities do not stay low at latitudes above 66.0° . Instead, an equatorward-moving density enhancement is observed. As can be seen in the density profiles at 0723 UT on Beam 10 in Figure 10, this ionization is at higher altitudes than that from proton precipitation, and thus indicates electron precipitation. Movement of the enhancement equatorward to the latitude of onset suggests that it might be the signature of an NS auroral form moving equatorward to the onset location as expected from the time sequence of *Nishimura et al.* [2010]. Unfortunately, for this event auroral imaging is not sufficient to evaluate this possibility further.

[32] A substorm onset at 0945 UT on 27 March 2007 (not shown) had a flow pattern similar to that in the previous event, a southeastward-directed flow enhancement moving equatorward that reaches onset latitude at approximately the onset time. A perturbation in the negative direction is also seen at lower latitudes where the flows were initially westward. In the 27 March 2007 case, considerable electron aurora within the radar E region fov prevented reliable detection of any possible signature of a reduction in the energy flux of precipitating protons.

4. Conclusions

[33] Taking advantage of the mapping of potential electric fields and associated flows from the plasma sheet to the ionosphere, we examined Poker Flat and Sondrestrom ISR observations for evidence of the flows inferred from the pre-substorm onset auroral sequence of *Nishimura et al.* [2010]. The time sequence starts with a PBI auroral enhancement expected to be associated with new plasma crossing the

outer boundary of the plasma sheet, the new plasma being suggested to enter the plasma sheet with enhanced flow and to have lower $PV^{5/3}$ than that of the pre-existing plasma sheet. We found such a flow enhancement within the 15 min period preceding onset for 19 of 36 substorm onsets identified during our nightside runs of the Sondrestrom radar. For only 6 of the onsets did we observe the absence of such a flow enhancement prior to onset. For some events, we also found evidence for E region density enhancement of a PBI associated with enhanced flow crossing the polar cap boundary. Such a flow enhancement is a signature of a localized enhancement of the reconnection rate along the outer plasma sheet boundary. Due to the lack of concurrent auroral observations, it is not feasible to determine whether any particular flow enhancement we observed was in fact associated with an onset. In addition, we could not determine whether a PBI and associated flow enhancement prior to any given onset were sufficiently well away from the radar longitude to not be seen by the radar. We thus conclude that flow enhancements as inferred by *Nishimura et al.* are commonly seen, and that the range of times ΔT before onset when the flow enhancements occur is essentially the same as seen by *Nishimura et al.* Although these observations offer support for *Nishimura et al.*'s inference that an enhanced flow of new plasma crossing the polar cap leads to onset, by themselves they do not provide definitive evidence that such flows lead to onset.

[34] We found further support, however, for the inferences of *Nishimura et al.* in observations with the Poker Flat ISR, which we used to look for the inferred flows within the equatorward portion of the auroral oval soon before onset and for evidence in E region densities that the flowing plasma has lower $PV^{5/3}$ than the surrounding plasma. We identified four events during our PFISR runs in which substorm onset occurred very close to or within the PFISR fov. Two of the onsets were associated with enhanced westward SAPS flows that began a few minutes prior to onset, which *Nishimura et al.* inferred to occur for onsets within the evening convection cell. For both examples, the E region densities clearly decreased at the same time as the flow enhancement and at the same latitudes at which the flow enhancement was seen. Such a decrease, occurring in the SAPS region, where the E region densities reflect ionization from proton precipitation, is consistent with what is expected if the plasma being brought to this region by the enhanced flows has lower $PV^{5/3}$ than the previous particle population. Note that the density decrease was not seen equatorward of the flow enhancement, indicating that low $PV^{5/3}$ plasma was not brought to the onset longitude prior to onset equatorward of the region of enhanced westward flows. In both cases, the flow enhancement and density decrease extended to the poleward boundary of the radar fov, whereas the auroral onset occurred somewhat poleward of this boundary. Thus we conclude that the auroral brightening at onset occurred poleward of at least some of the new plasma brought in by the enhanced flow, and the observations are consistent with formation of upward field-aligned currents near the poleward edge of the flows at onset.

[35] In the other two events seen by PFISR, a southeastward-directed flow enhancement was observed to move equatorward, reaching the onset latitude near the Harang reversal, at approximately the onset time. For one of the

events, the measured E region densities suggest that the plasma brought to the onset region by the enhanced flows had lower total flux tube $PV^{5/3}$ than the previous plasma population. The E region densities also give evidence of an NS aurora moving equatorward toward the onset region prior to onset. Such determinations could not be made for the second event because of electron auroral precipitation poleward of the onset region.

[36] In summary, the radar observations shown here give evidence that enhanced flows bring new plasma across the polar cap boundary and to the inner plasma sheet onset region, supporting the inferences from auroral ASI observations by Nishimura et al. [2010]. We also find consistency with the suggestion that the new plasma has lower entropy than the surrounding plasma, a suggestion that should be further evaluated with in situ observations. We also found evidence that auroral onset occurs to the right of the flow direction as illustrated by Nishimura et al. [2010, Figure 11]; this is consistent with the upward currents of the onset aurora being fed at least partially by ionospheric Pedersen currents flowing toward the aurora from within the flow channels bringing in the new plasma. It may also be important that E region densities for the two evening convection cell onsets considered here indicate the possibility that a decrease in $PV^{5/3}$ prior to onset occurs only within the region of enhanced westward SAPS and not equatorward of that region. This leads us to suggest that the intrusion of new plasma may reduce $PV^{5/3}$ only within the outer portion of the SAPS region proton population within the plasma sheet. Such a reduction would lead to an inward-directed perturbation in the radial gradient of $PV^{5/3}$ near the inner boundary of the intruding low $PV^{5/3}$ plasma. A perturbation in this direction is required for interchange instability [e.g., Xing and Wolf, 2007].

[37] **Acknowledgments.** This work at UCLA was supported by National Science Foundation grants ATM-0639312 and ATM-0646233 and NASA grant NNX09AI06G, and at UCLA and Berkeley by and NASA contract NAS5-02099. The Sondrestrom ISR and Poker Flat ISR measurements and analysis are supported under cooperative agreements ATM-0836152 and ATM-0608577, respectively, between the U.S. National Science Foundation and SRI International. We thank S. Mende and E. Donovan for use of the ASI data and the CSA for logistical support in fielding and data retrieval from the GBO stations. The Greenland magnetometer data used here were obtained from magnetometers operated by the Danish Meteorological Institute. The Canadian midlatitude magnetometer data used here were obtained from the CANMOS array operated by the Geological Survey of Canada. Alaska magnetometer data were obtained from Geophysical Institute of University of Alaska, Fairbanks.

[38] Bob Lysak thanks the reviewers for their assistance in evaluating this paper.

References

- Akasofu, S.-I. (1964), The development of the auroral substorm, *Planet. Space Sci.*, *12*, 273–282, doi:10.1016/0032-0633(64)90151-5.
- Anderson, P. C., W. B. Hanson, R. A. Heelis, J. D. Craven, D. N. Baker, and L. A. Frank (1993), A proposed production model of rapid subauroral ion drifts and their relationship to substorm evolution, *J. Geophys. Res.*, *98*, 6069–6078, doi:10.1029/92JA01975.
- Anderson, P. C., D. L. Carpenter, K. Tsuruda, T. Mukai, and F. J. Rich (2001), Multisatellite observations of rapid subauroral ion drifts (SAID), *J. Geophys. Res.*, *106*, 29,585–29,599, doi:10.1029/2001JA000128.
- Angelopoulos, V. (2008), The THEMIS Mission, *Space Sci. Rev.*, *141*(1–4), 5–34, doi:10.1007/s11214-008-9336-1.
- Angelopoulos, V., W. Baumjohann, C. F. Kennel, F. V. Coroniti, M. G. Kivelson, R. Pellat, R. J. Walker, H. Lüher, and G. Paschmann (1992), Bursty Bulk Flows in the Inner Central Plasma Sheet, *J. Geophys. Res.*, *97*(A4), 4027–4039, doi:10.1029/91JA02701.
- Auster, H. U., et al. (2008), The THEMIS fluxgate magnetometer, *Space Sci. Rev.*, *141*(1–4), 235–264, doi:10.1007/s11214-008-9365-9.
- Blanchard, G. T., L. R. Lyons, O. de la Beaujardière, R. A. Doe, and M. Mendillo (1996), Measurement of the magnetotail reconnection rate, *J. Geophys. Res.*, *101*, 15,265–15,276, doi:10.1029/96JA00414.
- Bristow, W. A. (2009), Relationship between substorm onset locations and nightside convection pattern features, *J. Geophys. Res.*, *114*, A12202, doi:10.1029/2009JA014576.
- Bristow, W. A., and P. Jensen (2007), A superposed epoch study of SuperDARN convection observations during substorms, *J. Geophys. Res.*, *112*, A06232, doi:10.1029/2006JA012049.
- Bristow, W. A., A. Otto, and D. Lummerzheim (2001), Substorm convection patterns observed by the Super Dual Auroral Radar Network, *J. Geophys. Res.*, *106*, 24,593–24,609, doi:10.1029/2001JA000117.
- Bristow, W. A., G. Sofko, H. C. Stenbaek-Nielsen, S. Wei, D. Lummerzheim, and A. Otto (2003), Detailed analysis of substorm observations using SuperDARN, UVI, ground-based magnetometers, and all-sky imagers, *J. Geophys. Res.*, *108*(A3), 1124, doi:10.1029/2002JA009242.
- de la Beaujardière, O., L. R. Lyons, and E. Friis-Christensen (1991), Sondrestrom radar measurements of the reconnection electric field, *J. Geophys. Res.*, *96*, 13,907–13,912, doi:10.1029/91JA01174.
- de la Beaujardière, O., L. R. Lyons, J. M. Ruohomäki, E. Friis-Christensen, C. Danielsen, F. J. Rich, and P. T. Newell (1994), Quiet-time intensifications along the poleward auroral boundary near midnight, *J. Geophys. Res.*, *99*, 287–298, doi:10.1029/93JA01947.
- Foster, J. C., and W. J. Burke (2002), SAPS: A new categorization for subauroral electric fields, *Eos Trans. AGU*, *83*(36), 393, doi:10.1029/2002EO000289.
- Heinselman, C., and M. J. Nicolls (2008), A Bayesian approach to electric field and E region neutral wind estimation with the Poker Flat Advanced Modular Incoherent Scatter Radar, *Radio Sci.*, *43*, RS5013, doi:10.1029/2007RS003805.
- Henderson, M. G., L. Kepko, H. E. Spence, M. Connors, J. B. Sigwart, L. A. Frank, H. J. Singer, and K. Yumoto (2002), The evolution of north-south aligned auroral forms into auroral torch structures: The generation of omega bands and ps6 pulsations via flow bursts, in *Sixth International Conference on Substorms*, edited by R. M. Winglee, pp. 169–174, Univ. of Wash., Seattle, Wash.
- Kim, H.-J., L. R. Lyons, S. Zou, A. Boudouridis, D.-Y. Lee, C. Heinselman, and M. McCready (2009), Evidence that solar wind fluctuations substantially affect the strength of dayside ionospheric convection, *J. Geophys. Res.*, *114*, A11305, doi:10.1029/2009JA014280.
- Lyons, L. R., T. Nagai, G. T. Blanchard, J. C. Samson, T. Yamamoto, T. Mukai, A. Nishida, and S. Kokobun (1999), Association between Geotail plasma flows and auroral poleward boundary intensifications observed by CANOPUS photometers, *J. Geophys. Res.*, *104*, 4485–4500, doi:10.1029/1998JA900140.
- Lyons, L. R., et al. (2009a), Evidence that solar wind fluctuations substantially affect global convection and substorm occurrence, *J. Geophys. Res.*, *114*, A11306, doi:10.1029/2009JA014281.
- Lyons, L. R., S. Zou, C. J. Heinselman, M. J. Nicolls, and P. C. Anderson (2009b), Poker Flat radar observations of the magnetosphere-ionosphere coupling electrodynamic of the earthward penetrating plasma sheet following convection enhancements, *J. Atmos. Terr. Phys.*, *71*, 717–728, doi:10.1016/j.jastp.2008.09.025.
- Maezawa, K., and T. Hori (1998), The distant magnetotail: Its structure, IMF dependence, and thermal properties, in *New Perspectives on the Earth's Magnetotail*, *Geophys. Monogr.*, vol. 105, edited by A. Nishida, S. W. H. Cowley, and D. N. Baker, p. 1, AGU, Washington, D. C.
- Mende, S. B., S. E. Harris, H. U. Frey, V. Angelopoulos, C. T. Russell, E. Donovan, B. Jackel, M. Greffen, and L. M. Peticolas (2008), The THEMIS array of ground-based observatories for the study of auroral substorms, *Space Sci. Rev.*, *141*(1–4), 357–387, doi:10.1007/s11214-008-9380-x.
- Nakamura, M., G. Paschmann, W. Baumjohann, and N. Sckopke (1991), Ion distributions and flows near the neutral sheet, *J. Geophys. Res.*, *96*, 5631–5649, doi:10.1029/90JA02495.
- Nakamura, R., W. Baumjohann, R. Schödel, M. Brittnacher, V. A. Sergeev, M. Kubyshkina, T. Mukai, and K. Liou (2001), Earthward flow bursts, auroral streamers, and small expansions, *J. Geophys. Res.*, *106*, 10,791–10,802, doi:10.1029/2000JA000306.
- Nishimura, Y., J. Wygant, T. Ono, M. Iizima, A. Kumamoto, D. Brautigam, and R. Friedel (2008), SAPS measurements around the magnetic equator by CRRES, *Geophys. Res. Lett.*, *35*, L10104, doi:10.1029/2008GL033970.
- Nishimura, Y., L. Lyons, S. Zou, V. Angelopoulos, and S. Mende (2010), Substorm triggering by new plasma intrusion: THEMIS all-sky imager observations, *J. Geophys. Res.*, *115*(A7), A07222, doi:10.1029/2009JA015166.

- Pilipp, W. G., and G. Morfill (1978), The formation of the plasma sheet resulting from plasma mantle dynamics, *J. Geophys. Res.*, *83*, 5670, doi:10.1029/JA083iA12p05670.
- Ritter, P., and H. Lühr (2008), Near-Earth magnetic signature of magnetospheric substorms and an improved substorm current model, *Ann. Geophys.*, *26*, 2781–2793, doi:10.5194/angeo-26-2781-2008.
- Robinson, R. M., and R. R. Vondrak (1985), Characteristics and sources of ionization in the continuous aurora, *Radio Sci.*, *20*(3), 447–455, doi:10.1029/RS020i003p00447.
- Sergeev, V. A., K. Liou, C.-I. Meng, P. T. Newell, M. Brittnacher, G. Parks, and G. D. Reeves (1999), Development of auroral streamers in association with localized impulsive injections to the inner magnetotail, *Geophys. Res. Lett.*, *26*, 417–420, doi:10.1029/1998GL900311.
- Sergeev, V. A., et al. (2000), Multiple-spacecraft observation of a narrow transient plasma jet in the Earth's plasma sheet, *Geophys. Res. Lett.*, *27*, 851–854, doi:10.1029/1999GL010729.
- Smirnova, N. V., A. N. Lyakhov, Y. I. Setzer, A. P. Osepian, C. I. Meng, R. Smith, and H. C. Stenbaek-Nielsen (2004), Precipitating protons and their role in ionization of the polar ionosphere, *Cosmic Res., Engl. Transl.*, *42*, 210–218, doi:10.1023/B:COSM.0000033296.08433.94.
- Stiles, G. S., E. W. Hones Jr., S. J. Bame, and J. R. Asbridge (1978), Plasma sheet pressure anisotropies, *J. Geophys. Res.*, *83*, 3166–3172, doi:10.1029/JA083iA07p03166.
- Wolf, R. A., Y. Wan, X. Xing, J.-C. Zhang, and S. Sazykin (2009), Entropy and plasma sheet transport, *J. Geophys. Res.*, *114*, A00D05, doi:10.1029/2009JA014044.
- Xing, X., and R. A. Wolf (2007), Criterion for interchange instability in a plasma connected to a conducting ionosphere, *J. Geophys. Res.*, *112*, A12209, doi:10.1029/2007JA012535.
- Zesta, E., E. Donovan, L. Lyons, G. Enno, J. S. Murphree, and L. Cogger (2002), Two-dimensional structure of auroral poleward boundary intensifications, *J. Geophys. Res.*, *107*(A11), 1350, doi:10.1029/2001JA000260.
- Zou, S., L. R. Lyons, M. A. McCready, and C. J. Heinselman (2008), High-time resolution dayside convection monitoring by incoherent scatter radar and a sample application, *J. Geophys. Res.*, *113*, A01203, doi:10.1029/2007JA012364.
- Zou, S., L. R. Lyons, C.-P. Wang, A. Boudouridis, J. M. Ruohoniemi, P. C. Anderson, P. L. Dyson, and J. C. Devlin (2009a), On the coupling between the Harang reversal evolution and substorm dynamics: A synthesis of SuperDARN, DMSP, and IMAGE observations, *J. Geophys. Res.*, *114*, A01205, doi:10.1029/2008JA013449.
- Zou, S., L. R. Lyons, M. J. Nicolls, C. J. Heinselman, and S. B. Mende (2009b), Nightside Ionospheric Electrodynamics Associated with Substorms: PFISR and THEMIS ASI Observations, *J. Geophys. Res.*, *114*, A12301, doi:10.1029/2009JA014259.
- Zou, S., L. R. Lyons, M. J. Nicolls, and C. J. Heinselman (2009c), PFISR observations of strong azimuthal flow bursts in the ionosphere and their relation to nightside aurora, *J. Atmos. Terr. Phys.*, *71*, 729–737, doi:10.1016/j.jastp.2008.06.015.

V. Angelopoulos, Department of Earth and Space Sciences, University of California, Los Angeles, CA 90095-1567, USA.

K.-H. Fornacon, Institut für Geophysik und Extraterrestrische Physik, Technische Universität Braunschweig, D-38106 Braunschweig, Germany.

C. Heinselman and M. J. Nicolls, Center for Geospace Studies, SRI International, Menlo Park, CA 94025, USA.

H.-J. Kim, L. R. Lyons, and Y. Shi, Department of Atmospheric and Oceanic Sciences, University of California, Los Angeles, CA 90095-1565, USA. (larry@atmos.ucla.edu)

Y. Nishimura, Solar-Terrestrial Environment Laboratory, Nagoya University, Nagoya, Aichi 464-8601, Japan.

S. Zou, Department of Atmospheric, Oceanic and Space Sciences, University of Michigan, Ann Arbor, MI 48109, USA.